Beyond 300°C: Reliable Long-Term Measurement of Temperature for Supercritical Geothermal Systems

William Jacobsen¹, Ricardo Vanegas², John D'Urso¹, Abdel Soufiane¹, David Payne¹, Dana Dutoit¹, Gregor Cedilnik², and Farhan Zaidi²

¹AFL (USA)

²AP Sensing (Germany)

Keywords

High temperature, supercritical, DTS, FIMT, optical fiber, Raman backscattering

ABSTRACT

The geothermal industry has been attempting to tap "supercritical" wells since the early 1980s. Temperature is a key parameter within these wells because it directly relates to energy potential.

Fiber optic technology has been used extensively in the oil and gas industry to provide important communications and sensing functions for reservoir management. Distributed temperature sensing (DTS) systems, which use optical fibers to measure temperature along the entire length of the installed fiber, have been used for complete well profiling at temperatures up to 300°C. To expand into the monitoring of supercritical geothermal systems beyond 300°C, new optical fibers and cable structures are required to allow these distributed temperature systems to perform.

A low attenuation metal-coated optical fiber and cable capable of withstanding temperatures up to 500°C will be demonstrated in this work. Performance will be validated by using a DTS instrument to measure temperature readings.

1. Introduction

Supercritical geothermal systems are those in which the temperature and pressure exceed 374°C and 221 bar respectively (Elders et al., 2003). The potential ability of these wells to deliver up to 10 times the power of a "normal" well (Palsson et al., 2011) has led to a number of ongoing projects throughout the world (Dobson et al., 2017).

It is necessary to develop instrumentation and sensors to characterize and exploit these supercritical reservoirs. Because it is directly related to the energy potential, temperature is a

key parameter (Massiot et al., 2010). Both fiber optic distributed temperature sensing (DTS) and wireline techniques have been examined. While there has been some success in developing wireline instruments, commercial instruments cannot operate beyond 300°C and experimental ones are not rated above 400°C (Asmundsson et al., 2014). It may be noted that a slick-line logging tool was developed which was capable of measuring 450°C; however, its capability to withstand such high temperatures appears limited to approximately 8 hours (Dobson et al., 2017). In summary, no clear solution has been presented for logging geothermal wells at temperatures above 400°C (Normann and Glocka, 2014), while it is expected that future instruments will likely need to tolerate temperatures up to 600°C (Asmundsson et al., 2014).

Distributed Temperature Sensing (DTS) was first applied to a geothermal well in 1992 (Benoit and Thompson, 1998). Initially used at lower temperatures, their use was extended to higher temperatures by applying learning gained through use in the oil and gas industry (Sanders and MacDougall, 2009). This allowed usage up to 300°C. Application to higher temperature is hindered by two predominant issues. The first is hydrogen darkening which is the increase of optical loss due to the absorption of hydrogen into the optical fiber (Palit et al., 2012). The second is degradation of the commonly used polyimide coating of the fiber (Benoit and Thompson, 1998).

DTS instruments require calibration before being deployed; high temperature calibration is required to achieve proper temperature accuracy in high temperature applications (SEAFOM, 2016). In addition, it is expected that at extreme temperatures, significant optical losses will occur. These optical losses have a direct relationship to temperature resolution; as optical loss increases, temperature resolution decreases exponentially (SEAFOM, 2016).

For temperatures above the rating of many polyimide coated fibers (> 300°C), metal coatings would be attractive. Those produced to date have been deemed unsuitable for geothermal well deployment due to high attenuation values at low temperatures (Reinsch and Henninges, 2010). This attenuation as well as significant attenuation changes during cycling is generally attributed to micro-bending and the large mismatch of the coefficients of thermal expansion between the metal coating and the glass fiber (Bogatyrev and Semjonov, 2007). Among other things, thinner metal coatings could help to mitigate these issues; however, the production of long lengths of high quality metal-coated fiber with controlled thickness of the coating is non-trivial (Bogatyrev and Semjonov, 2007).

2. Fiber/Cable Design

2.1 Glass Chemistry and Hydrogen Resistance

It has been demonstrated since the early 1980s that hydrogen ingression in silica-based glass induces losses in optical fibers at specific wavelengths due to the absorption of a variety of hydrogen related species (Stone, 1982). Depending on the application conditions such as temperature, partial pressure of H_2 and exposure time, absorption peaks can originate from two sources: free molecular hydrogen dissolved in silica, and the reaction of hydrogen with the various defects in the core of fiber (Noguchi, 1985).

Common silica fibers used in communications such as standard single-mode (SM) and standard graded-index multimode (MM) suffer a dramatic optical degradation in presence of hydrogen even at room temperature. The cores of these fibers are typically doped with refractive index increasing elements such as germanium and phosphorus. Depending on the temperature and H₂ concentration, once hydrogen diffuses in the fiber core, it can migrate to interstitial sites of the structure and/or bond with existing defects in the glass such as SiO, GeO and P-O. Figure 1 shows the growth of H₂ related peaks in the 800-1600nm spectral range for a typical GeO₂-P₂O₅ doped silica fiber (Allard, 1990). The overall fiber loss reached hundreds of decibels per kilometer, which makes it unusable for any light transmission applications.

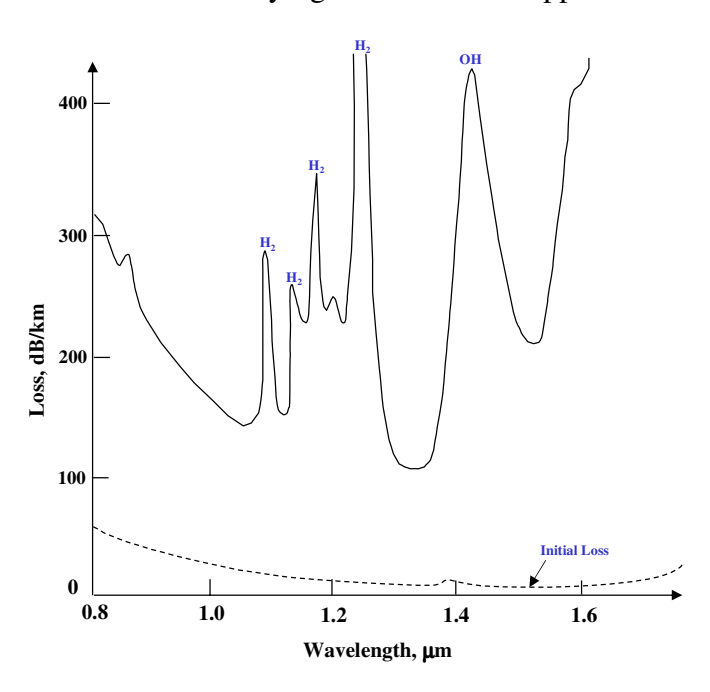


Figure 1: Spectrum of a Ge/P doped GI-MMF before and after exposure to <1atm of H₂ at ambient (Allard, 1990)

In Figure 1, it can be seen that although all wavelengths are impacted by H₂-induced loss, some wavelengths are more affected than others. A detailed explanation of how DTS works appears later in this paper, but suffice it to say that DTS results will be adversely affected if the fiber experiences loss changes at the operating wavelength due to any extrinsic effects such as hydrogen-induced loss; it is impossible to segregate the contribution of hydrogen to the temperature reading from that of the actual temperature change. Due to the possible appearance of these H₂ related peaks, many Raman-based DTS instruments operate at 1064nm. Figure 2 shows the H₂-induced loss of a standard Ge-doped graded-index multimode fiber at 1064nm under 143psi of pure H₂, 150°C for 800 hours.

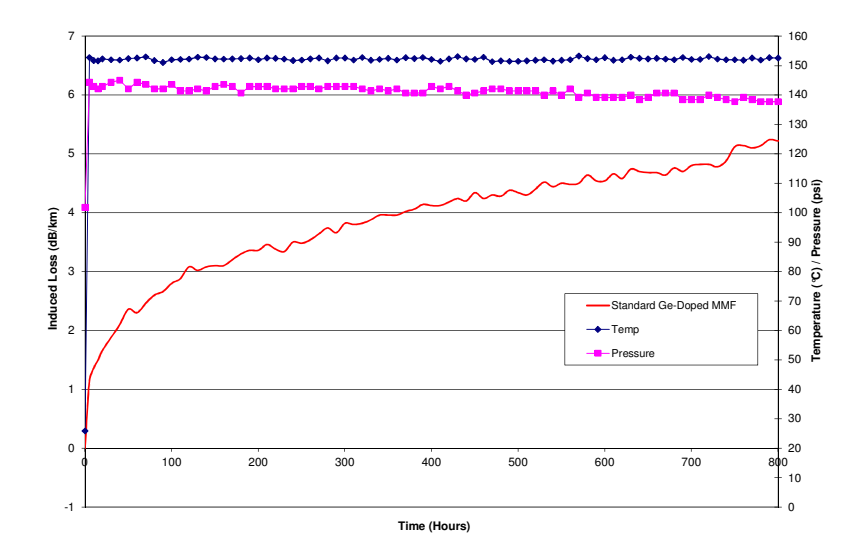


Figure 2: H₂-induced loss of Ge-doped GI-MMF at 1064nm under 143psi of pure H₂, 150°C for 800 hours.

It is clear from Figure 2 that the loss induced by hydrogen ingression continues to rise over time with a slope that indicates that no saturation is occurring. This continuous loss increase is detrimental to DTS measurement, so preventing hydrogen from diffusing in glass and bonding with defects in the fiber core is the only solution to achieve a meaningful reading of temperature using Raman-based DTS systems.

One way of creating a barrier to hydrogen in optical fibers is the application of a hermetic coating on the surface of the glass. Many different coatings have been explored, e.g. metals, ceramics, and carbon (Lemaire, 1991). Ceramic coatings such as silicon nitride or silicon carbide have been used, and have demonstrated to be effective in providing resistance to water at elevated temperatures and pressures but their mean strength is significantly below the value for standard polymer coated glass fibers and makes them highly impractical (Duncan, 1981).

Carbon coatings on the other hand appear to be the most attractive in providing solutions to the above mentioned problems for temperatures in excess of 100° C; at these temperatures e.g., saturation lifetimes with respect to hydrogen ingression are on the order of years; micro-bending is minimal and mean strength while on average is still below the optimal values obtained for polymer coated fibers, is very sufficient for most applications (Wang 2004). Figure 3 shows the effects of hydrogen in unprotected MM fibers and the benefit of carbon coating as a barrier to H_2 in the same fiber type.

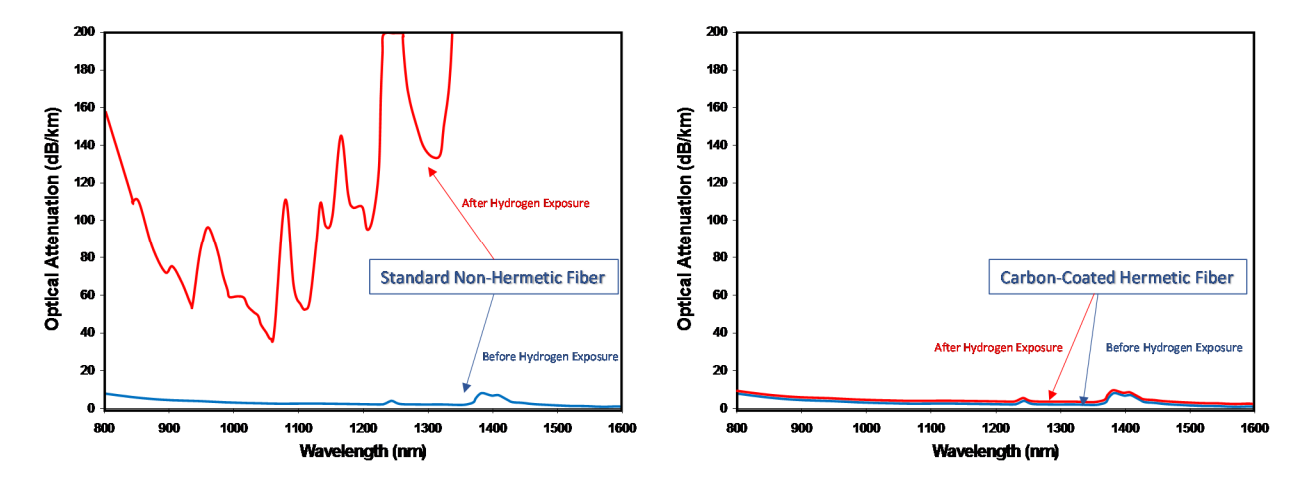


Figure 3: (Left) Standard GI-MMF before / after H₂ exposure (Right) Hermetically-sealed GI-MMF before / after H₂ exposure. Tests performed under 1500psi pure H₂, 200°C, for 17 hours.

AFL's Verrillon® carbon coating has proven to be a true barrier against hydrogen and moisture up to 170°C, covering numerous applications in the harsh environment industries. However, for applications requiring temperatures above 170°C, the effectiveness of carbon as a hydrogen barrier starts to diminish, and at temperatures above 200°C, the carbon layer becomes more permeable to hydrogen (Sanders and MacDougall, 2009).

To expand the use of optical fiber to temperatures greater than 170°C, AFL took an innovative approach to prevent the optical degradation of optical fibers immersed in a harsh environment by modifying and optimizing the design of the glass component of the fiber itself, independently of the properties (or even the presence) of the hermetic coating. In particular, the approach consists of eliminating the dopants that create more defects in the glass structure such as germanium, phosphorus, and boron. The fiber is designed with only silica in the core, along with fluorine doping to achieve the graded index profile of the multimode fiber (Weiss, 2005). This fiber is produced by AFL and is branded as Verrillon® VHM5000; it is a 0.2 NA 50/125µm GI-MMF. Figure 4 shows the performance of VHM5000 polyimide coated fiber at 1064nm under 1500psi of pure H₂, 200°C for 160 hours – without carbon coating.

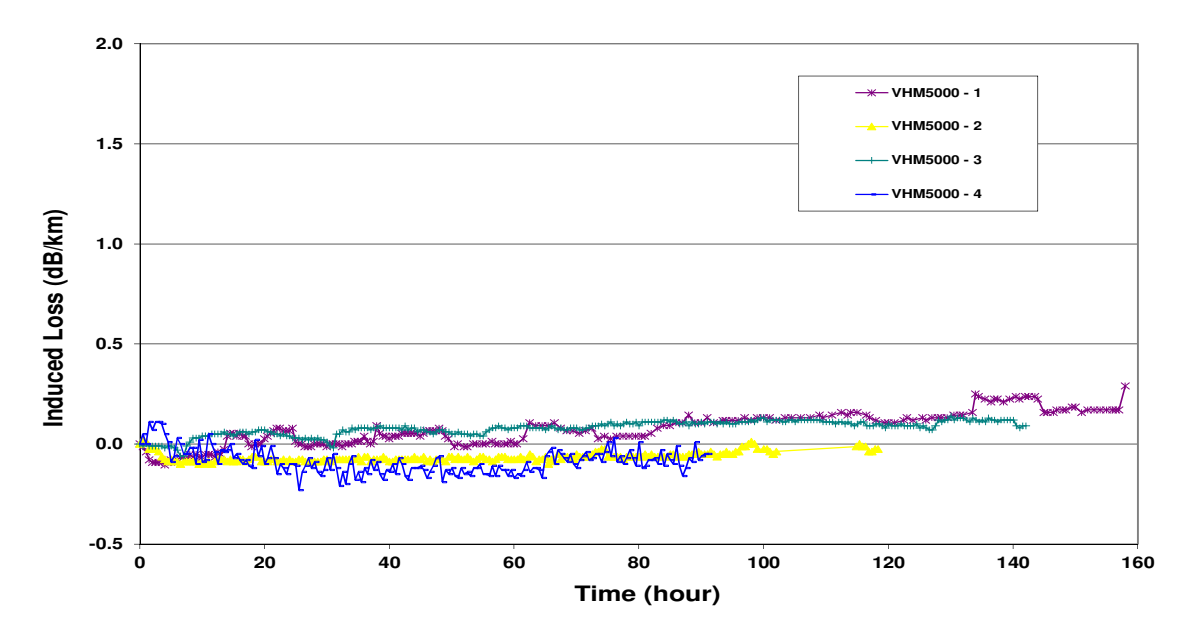


Figure 4: Performance of VHM5000 polyimide coated fiber at 1064nm under 1500psi pure H₂, 200°C for 160 hours

VHM5000 has historically performed exceptionally well in temperatures as high as 300°C, and under hydrogen pressures as high as 100atm.

2.2 Metallic Fiber Coating

The fiber used in this trial had a gold based coating with a thickness of approximately 3 - $5~\mu m$ which is well below the typical coating thickness of $15-25~\mu m$ for commercially available metal-coated fibers. A cross-sectional SEM image demonstrating the good concentricity and integrity of the coating process is shown in Figure 5.

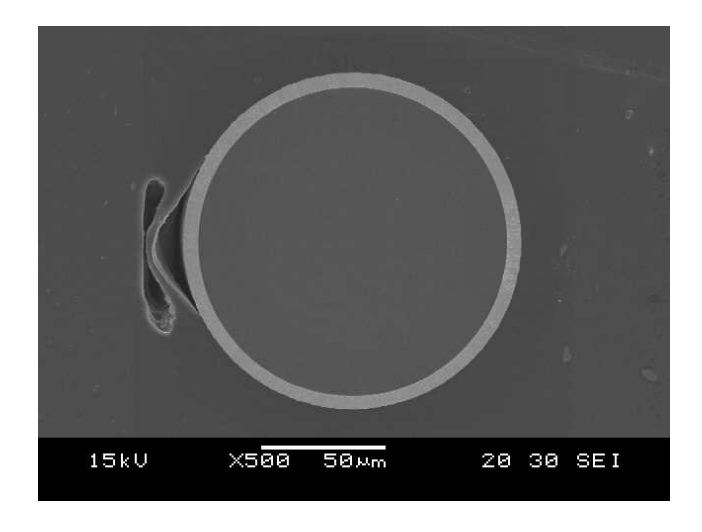


Figure 5: SEM cross-section of fiber produced using the current process

Metal-coated fibers can have optical losses in as-drawn condition as high as 20–100 dB/km at room temperature (Bogatyrev and Semjonov, 2007). Figure 6 shows the spectral attenuation of VHM5000 with a gold-based coating as shown in Figure 5, at room temperature, measured on 88m of fiber. Fiber was in a 300mm diameter loose coil.

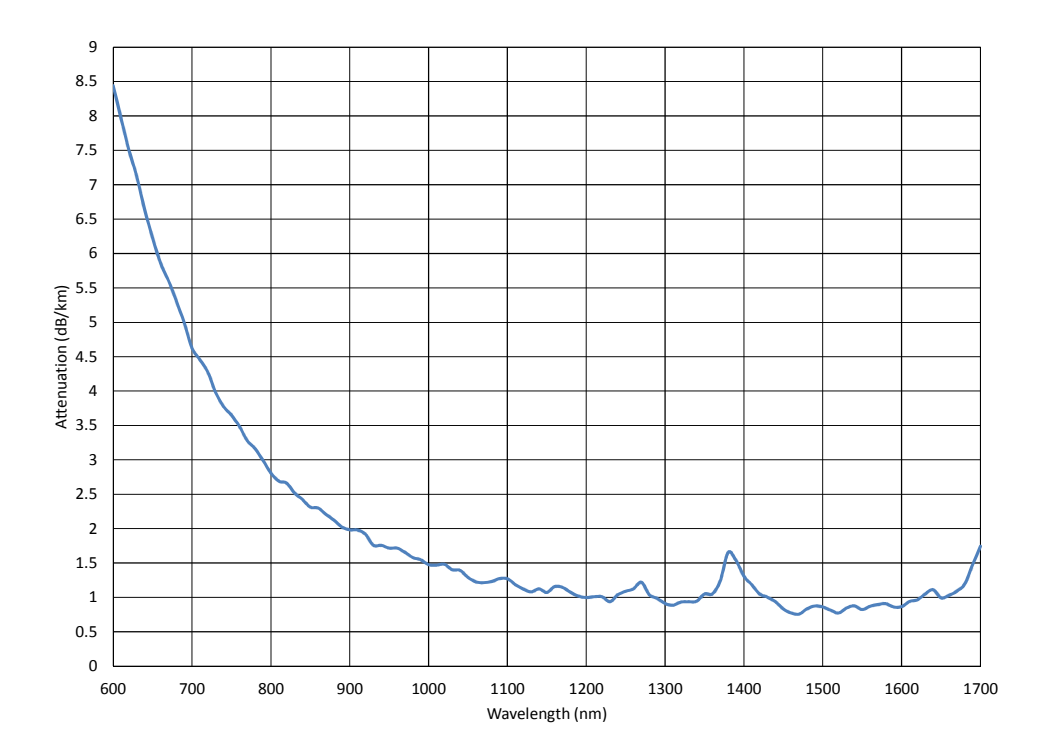


Figure 6: Spectral attenuation of VHM5000 with gold-based coating, 88m long, 300mm diameter loose coil, room temperature

The spectral attenuation of this fiber with a gold-based coating shows attenuation levels similar to standard acrylate or polyimide coated multimode fibers, as opposed to the significantly higher levels shown by other commercially available metal-coated multimode fibers.

2.3 Cabling

The cable of this study was constructed by producing a continuously welded Stainless Steel tube in 316 alloy via a roll forming / continuous laser welding process.

The starting material is 316 Stainless Steel strip in a width and thickness appropriate to produce the desired tube outside diameter of 2.78mm; this strip is fed through a set of forming rolls to produce a round tube profile with an open seam uppermost. This seam is sealed using a high power laser welding process to produce a continuous seam weld along the length of the tube.

Two of AFL's Verrillon® metallically-coated VHM5000 optical fibers, 100m in length each, were surface treated (patent pending) then introduced into the tube during this forming process. The finished tube undergoes a process to increase the excess fiber length (EFL) in the tube to ensure that there is adequate fiber present to accommodate the thermal expansion that the tube will see in service.

At the start of processing, a cross section of the welded tube is examined to verify that adequate weld penetration has been achieved; once this is verified, the fiber is introduced into the tube and processing can proceed. After completion on the production run a tensile sample of the tube is pulled to validate that the desired physical properties of the tube have been obtained and a twist test comprising multiple 180 degree twists of a constrained tube sample is carried out to validate the strength of the longitudinal seam weld. Twenty such twists without seam failure is deemed acceptable.

3. Raman Distributed Temperature Sensing (DTS)

A Raman DTS compares the intensity of the Raman "Stokes" and "Anti-Stokes" backscatter down the length of an optical fiber. These intensities have a defined relationship for a given medium (in this case, silica fiber) which is temperature dependent (Bolognini and Hartog, 2013). This allows the derivation of the temperature down the length of the fiber from the ratio of their intensities (Soto et al., 2011). According to Raman theory, one coefficient in that relationship is the frequency shift of the Raman backscatter with respect to the stimulus pulse frequency inserted by the DTS measurement (Stoddart et al., 2005).

For this test, the N4386B Linear Pro Series DTS instrument from AP Sensing was used, which exploits the functionality of Optical Time Domain Reflectometry (OTDR). This instrument operates at a wavelength of 1064nm, where fibers usually show lower hydrogen darkening compared to the other wavelengths commonly used in telecommunications (Kimura et al., 2001).

The DTS instrument can compensate for optical loss differences between Stokes and Anti-Stokes backscatter signal (which causes a slope in the temperature curve) by measuring the fiber from both ends, i.e. along opposite directions. This is known as a "double-ended" measurement. By combining both results (one mirrored along the distance axis) such effects cancel out, leading to significantly improved temperature accuracy (Fernandez et al., 2005). Using a special algorithm (patent pending) implemented for this trial, the best quality data is used for each fiber location while maintaining the cancelling-out benefit of the double-ended approach. This leads to consistently good temperature resolution along all fiber locations.

In addition, a novel method of calibration was employed for this trial. The High Temperature Calibration (HTC) implemented for this test takes individual calibrations of the effective Raman frequency shift parameter from the factory to minimize such non-linearity. This factory calibration was not performed with the fiber used in this trial (which would be optimal), but it compensates the instrument's individual effect from the receiver path. The addition of the HTC while operating in double-ended mode makes this instrument suitable for applications where wide temperature ranges need to be measured and where fiber / cable properties can vary over time. Gain and offset are still required to be adjusted at the highest expected temperature measurement and extend down to room temperature.

4. Test Protocol

The oven used was a Sentro Tech ST-1200C-363636 High Temperature Box Furnace with a Yudian 708P controller. The heating chamber size is 36-inch x 36-inch x 36-inch. The oven does not have a chiller so it cools down as fast as the ambient environment will allow it to. The test was conducted in air; neither the furnace nor the cable were purged during the test.

The cable was in a "loose coil" configuration of around 18-inch diameter, placed on a rack at the base of the oven. On a rack one foot above the loose coil, one section of cable was fixed via metal tie-wrap in an S-shape with two (2) 12-inch diameter tight bends matching the specified minimum bend radius of this cable design (Figure 7). Both ends of the cable exited the top of the oven.



Figure 7: Cable configuration inside oven

Above the rack was a thermocouple port; a K-type thermocouple was inserted through the port, which was connected to a calibrated Omega HH309A Four-Channel Temperature Data Logger. The data logger was programmed to collect a data point every 15 minutes.

Only one of the two optical fibers in the cable was to be interrogated by the N4386B unit; the second fiber was for redundancy in case of failure. Both ends of the fiber were spliced to connectorized pigtails, which allowed the connection to the DTS unit. Having both ends of each fiber connectorized allowed the DTS unit the option of performing "single-ended" or "double-ended" measurements. The DTS measurement sequence consisted of two (2) single-ended configurations from each end of the fiber and one (1) double-ended configuration combining both ends of the fiber. A laptop computer, which was connected to the DTS instrument at all times, was used to configure and gather the temperature traces generated by the unit.

In a constant, room-temperature controlled environment, and with a configuration of 2.0m spatial resolution / 600s measurement time, the DTS instrument can maintain a temperature resolution of 0.05°C. Due to the short length of the fiber (100m), it was decided to improve the spatial accuracy by reducing the spatial resolution to 1.0m. This, in turn, increased the expected

temperature resolution of the DTS instrument to 0.10°C. Single-ended measurements were completed with a measurement time of 60s each, while the double-ended measurement was completed with a measurement time of 120s. The total measurement time for the sequence was 240s.

The Yudian 708P controller is a fairly simple controller, capable of performing 50 steps maximum. Therefore, the testing was broken out into two tests. The first test performed basic cycling, along with a long-term soak at 500°C (Figure 8); the goal was to validate cable / fiber performance. Each cycle took 48 hours; the long-term soak at 500°C was 167 hours. The second test ramped up to 500°C, then went down to room temperature very slowly, over a matter of days, to better illustrate N4386B DTS performance over a wide temperature range (Figure 9). The temperature ramp rate for the first test was 30°C / hour; this was slow enough to not cause shock to the fiber, while also allowing the oven to be able to cool down and follow a consistent temperature profile. For the second test, the initial temperature ramp-up was 30°C / hour, while the cool down ramp rate was a slow 3°C / hour, in order to evaluate how the DTS instrument performed. The fiber was soaked for 12 hours at 250°C, 200°C, and 150°C.

At the start of the first test, when the thermocouple temperature reached 500°C, the gain of the N4386B was adjusted so the DTS temperature measurements would match the thermocouple temperature measurements. That was the only time any change was made to how the DTS unit processed data for the duration of the first test. At the completion of the first part of the test, the DTS unit was returned to Germany.

For the second part of the test, a different N4386B serial production unit with High Temperature Calibration was used. For this second unit, the gain was once again adjusted once the temperature reached 500°C.

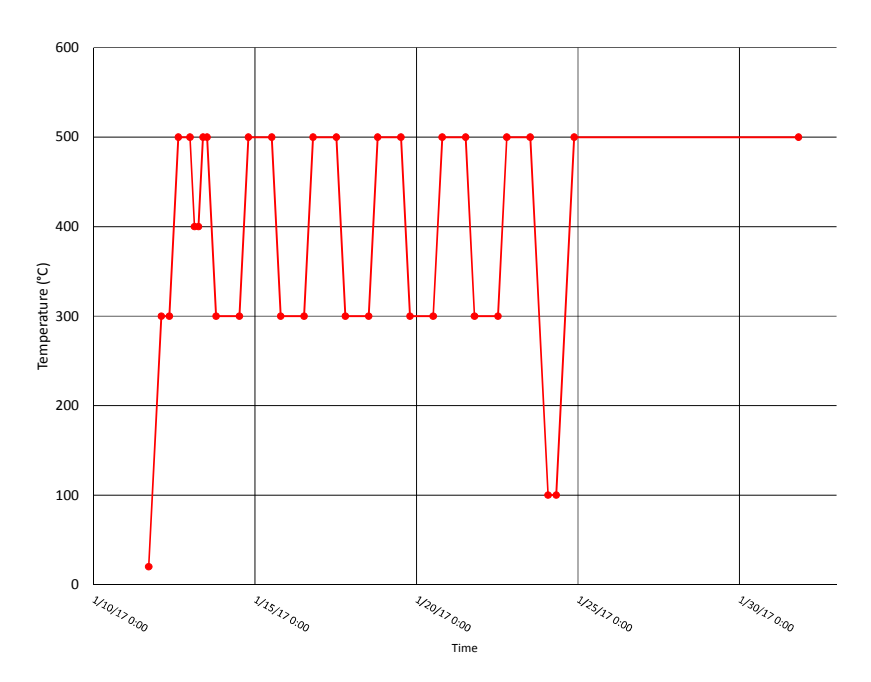


Figure 8: Oven – programmed temperature profile, first test (cycling)

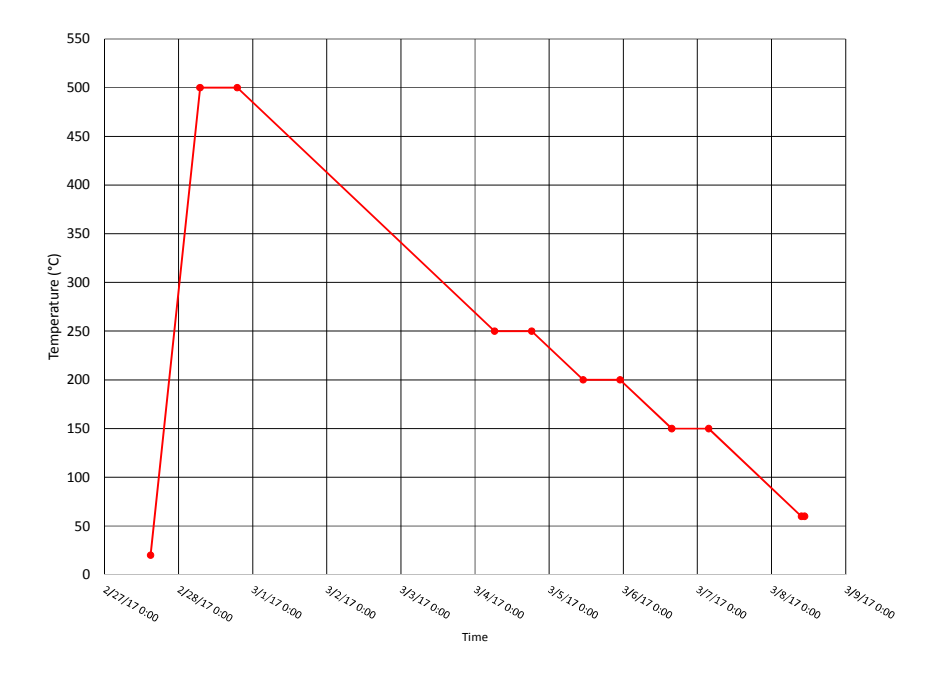


Figure 9: Oven - programmed temperature profile, second test (DTS performance)

5. Results

Figure 10 shows the results of the first test, thermocouple vs. DTS measurement, for the entire temperature profile as shown in Figure 8. The DTS temperature is the average temperature along the fiber from position 30m to position 110m. Both the DTS resolution and the thermocouple resolution are the standard deviation of the temperature over 50 points in time. The calculated temperature resolution is a combination of the instrument's noise and the temperature oscillation within the oven due to the temperature control cycle.

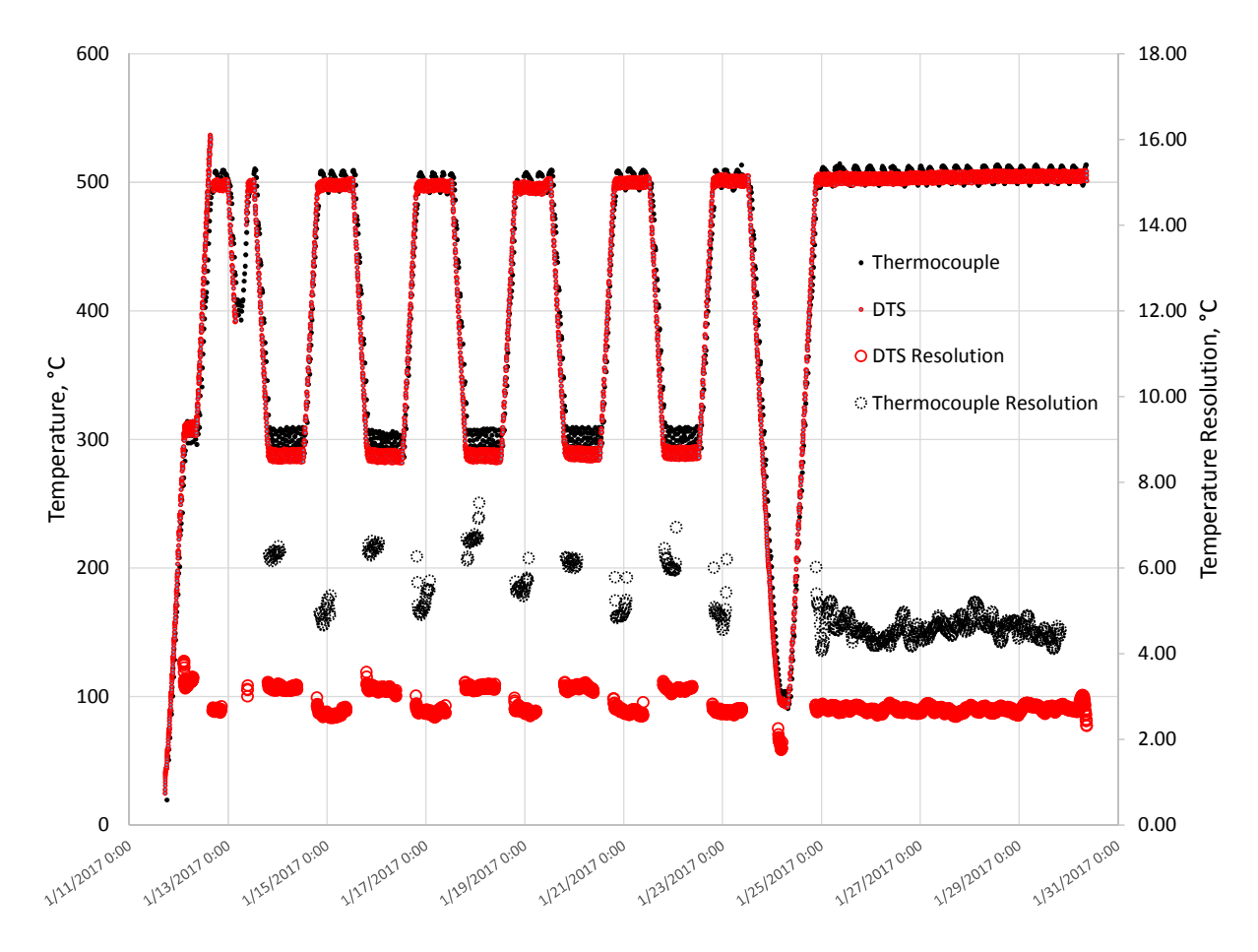


Figure 10: Temperature of thermocouple data logger vs. DTS N4386B, double-ended measurement, 300°C to 500°C cycling intervals (first test)

Figure 11 shows the results of the second test, thermocouple vs. DTS measurement, for the temperature profile from 500°C down to room temperature as shown in Figure 9, with an additional temperature excursion to 200°C.

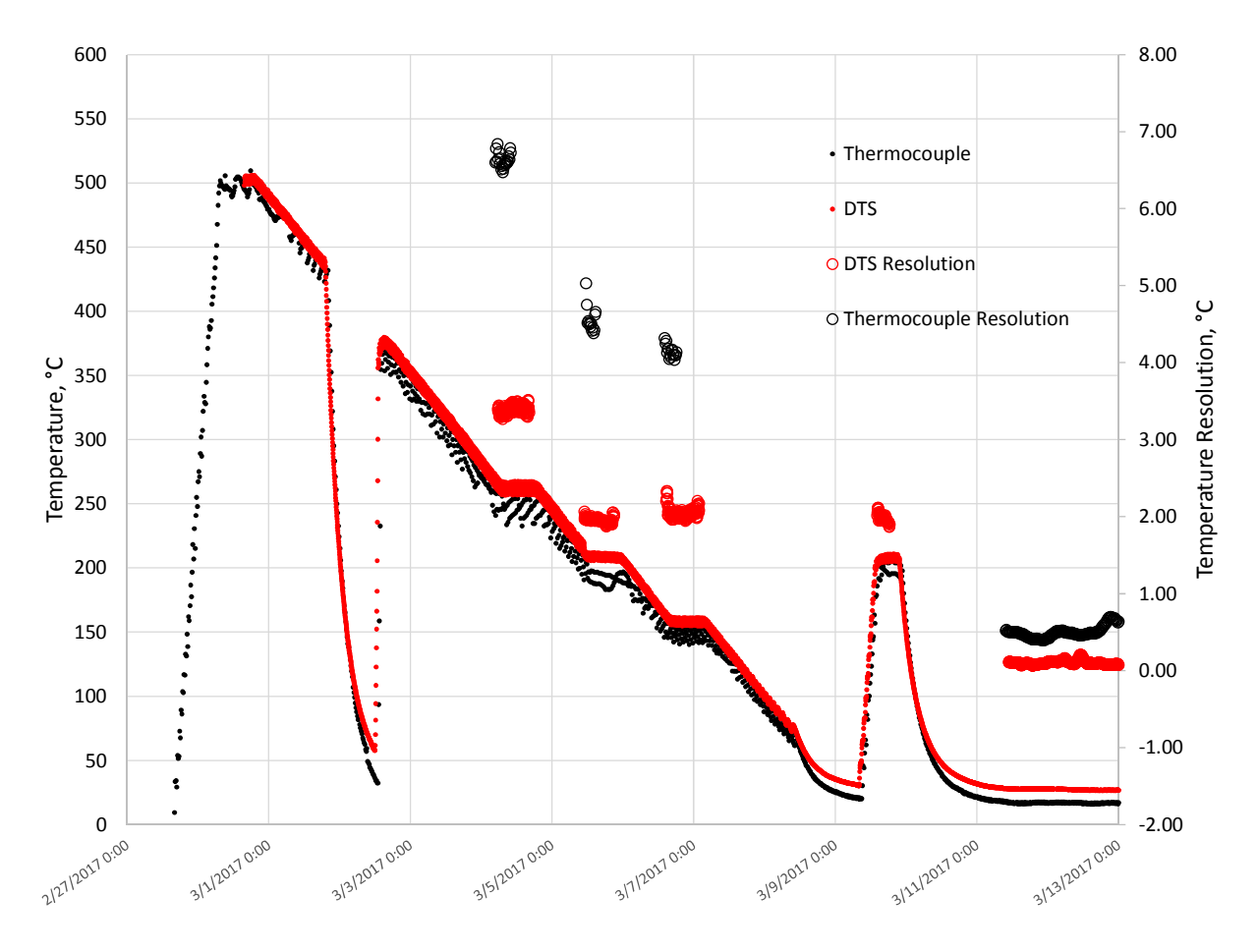


Figure 11: Temperature of thermocouple data logger vs. DTS N4386B, double-ended measurement, soaks at 500°C, 250°C, 200°C, 150°C, and room temperature (second test)

Figure 12 shows an expanded section of Figure 10, during the extended 500°C soak at the end of the first test.

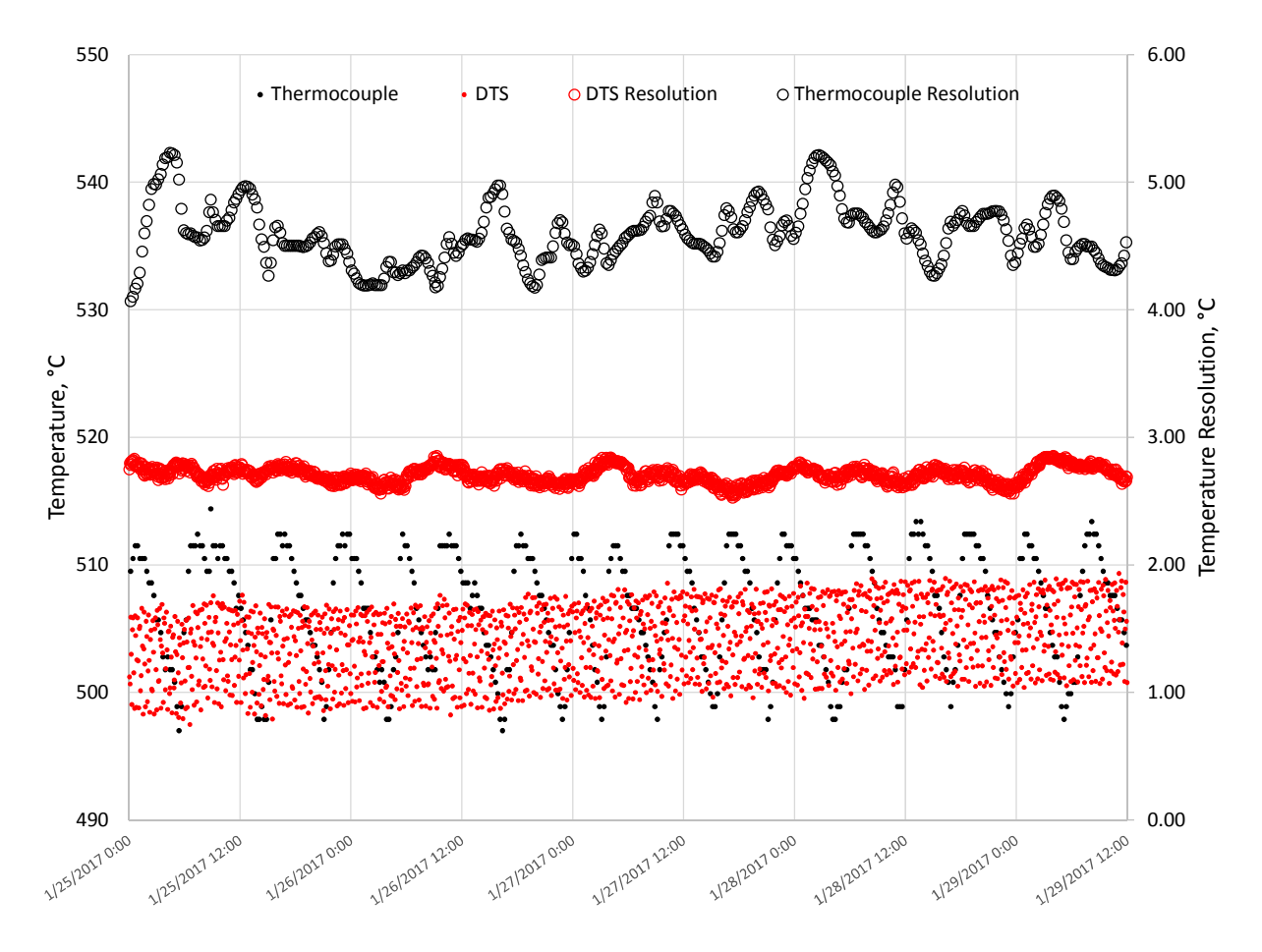


Figure 12: Temperature of thermocouple data logger vs. DTS N4386B, double-ended measurement, 500°C soak (end of first test)

Figure 13 shows an expanded section of Figure 11, during the room temperature soak at the end of the second test.

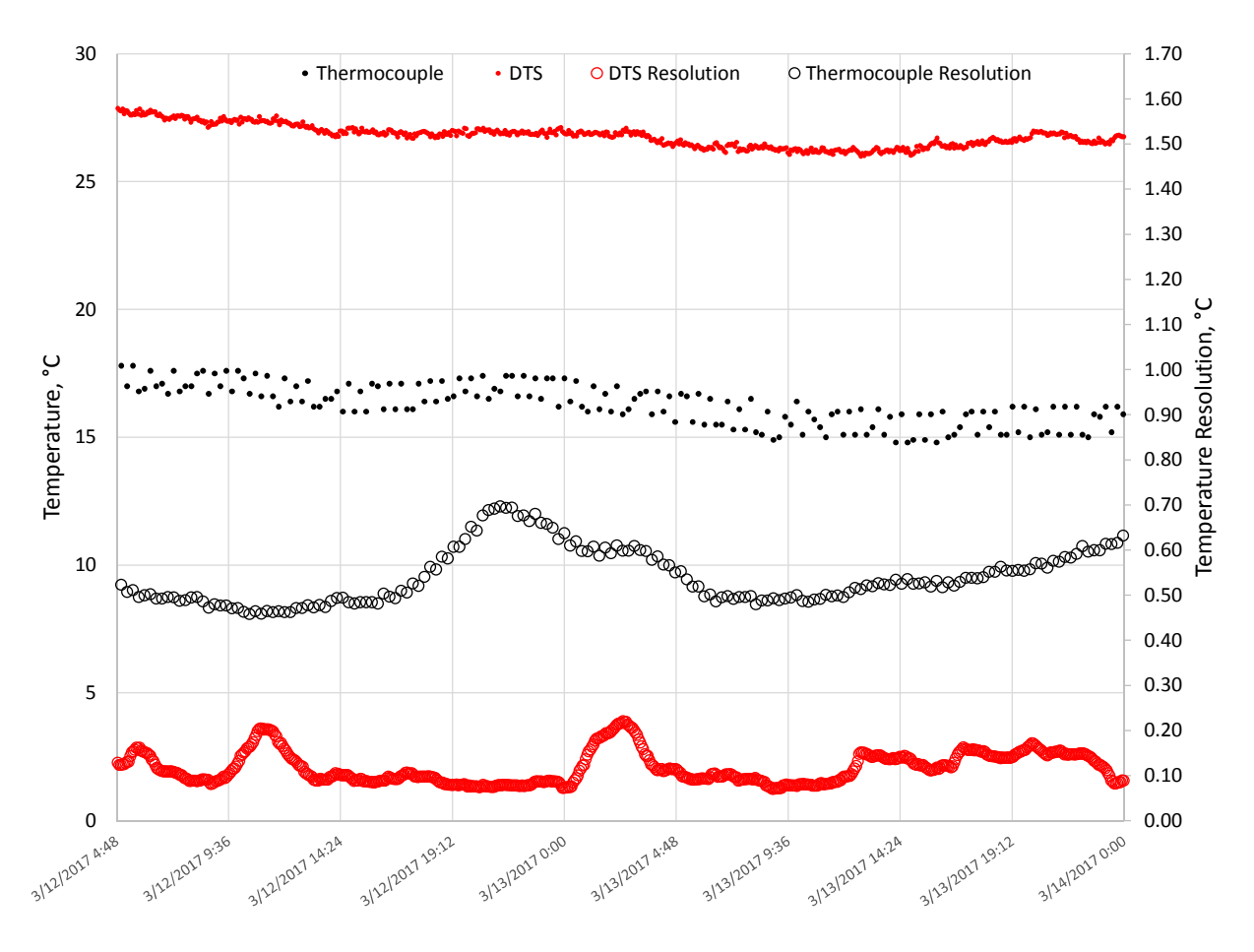


Figure 13: Temperature of thermocouple data logger vs. DTS N4386B, double-ended measurement, room temperature soak (end of second test)

6. Discussion

Figures 10 and 11 show that both the thermocouple and the DTS consistently matched the temperature profile in Figures 8 and 9. The only adjustment made on either of the N4386B units was the adjustment of the gain once temperature reached 500°C at the first cycle for each test section. In Figure 11, the DTS instrument was not data logging temperature until after the calibration was completed, which is why there is no DTS data on the initial temperature ramp. In addition, there was a power outage which caused a significant disruption in the expected temperature profile. It is important to note that the temperature decrease (and subsequent increase) was 'uncontrolled', and the cable, fiber, and DTS continued to perform well during and after the temperature glitch.

Figure 12 clearly shows how the N4386B performs compared to the thermocouple during the 500°C soak on the first test. The DTS data can be seen to be between the max / min values recorded by the thermocouple data logger. This shows that the gain value set at the beginning of the test at 500°C was still accurate after the multiple temperature cycles were performed. It also makes it easy to see how the temperature resolution of the DTS is better than the thermocouple resolution.

However, the temperature data in Figure 12 makes it appear as if the DTS data is noisy. The thermocouple was logging a temperature measurement every 15 minutes. In looking at Figure 12, it would appear that the oven cycles between maximum and minimum temperature approximately every 6 hours. After the conclusion of the trial, the oven was run at 500°C again while logging a temperature measurement every minute. Figure 14 shows a subset of Figure 12, with the new data overlaid with the old data.

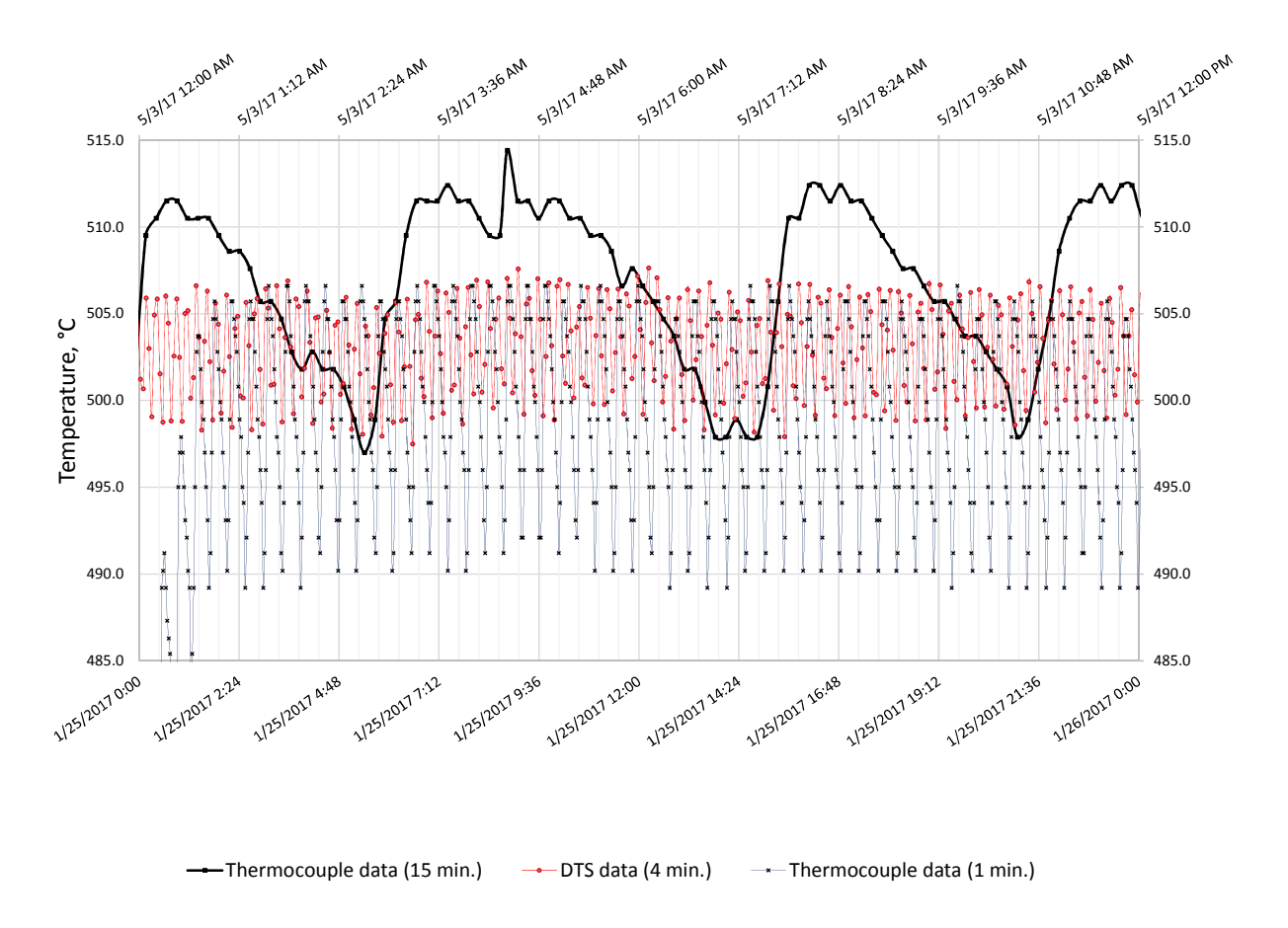


Figure 14: Oven temperature at 500°C, with additional thermocouple logger data (measurement taken every minute)

The new thermocouple data shows that the oven actually cycles between maximum and minimum temperature approximately every 13 minutes as opposed to every 6 hours. According to the Nyquist – Shannon Sampling Theorem, the thermocouple data logging should have been recording samples every 6 ½ minutes instead of every 15 minutes. Since the DTS sequence measurement period was 4 minutes, the DTS was able to capture the oscillation of the oven temperature – and therefore, appeared noisier than the thermocouple data.

Figure 13 makes a number of interesting points. First, it can be seen that the DTS temperature at 'room temperature' is not quite room temperature; the thermocouple temperature is around 17°C, while the DTS temperature is around 27°C. This difference is due to the gain change made on the N4386B at 500°C; had the gain change not been made at 500°C, the DTS temperature would

have been about 530°C, resulting in a 30°C offset. By changing the gain at 500°C, it can be seen that at room temperature, there is only a 10°C offset.

The data shown in Figure 13 was also used to confirm that the changes made to the N4386B to support this trial were working (1m spatial resolution, 0.1°C temperature resolution at room temperature). For all the different regions of the tests where temperature was maintained constant, a fifty-point (50) standard deviation (moving average) was calculated and used as the temperature resolution of the measurement. The following temperature resolutions were obtained at the different temperature steps:

Temperature	Temperature Resolution	Percent of Temperature
Room Temp / ~ 25°C	< 0.1°C	< 0.4%
150°C	< 2.0°C	< 1.3%
200°C	< 2.0°C	< 1.0%
250°C	< 3.5°C	< 1.4%
300°C	< 3.5°C	< 1.1%
500°C	< 3°C	< 0.6%

This confirms that the changes made to the N4386B to support this trial performed as expected. In addition, had the factory calibration of the DTS unit been performed with the fiber used in this study, the accuracy of the temperature measurement could have been further improved.

7. Conclusion

A low attenuation metal-coated optical fiber and cable capable of withstanding temperatures up to 500°C was demonstrated. Performance was validated using the N4386B DTS instrument from AP Sensing. The DTS showed that it was able to accurately and consistently record temperatures across multiple temperature cycles, during extended high temperature soak periods, and over the temperature range from 25°C to 500°C.

At the conclusion of the study, the cable was dissected and examined in 1m increments. It was found that the tube retained its integrity throughout the test. Parts of the tube that were heated in the chamber were subjected to the same test used to validate the strength of the longitudinal seam weld when the tube was initially welded; the heated tube passed the twist test. The fibers did not stick to the inside of the tube, or to each other.

The results demonstrate that metal-coated fibers and suitable DTS instruments can be deployed in supercritical geothermal systems to provide accurate temperature information.

8. Acknowledgements

The authors would like to acknowledge the significant contributions provided by the AFL Quality Control department, specifically from Sarah Kendrick, Lonnie Phillips, and Larry Zahm, without whom this trial could not have been successful.

REFERENCES

- Allard, F.C. "Chapter 1: Optical Fibers." *Fiber Optics Handbook: For Engineers and Scientists*. New York,NY: McGraw-Hill, (1990), 1.27.
- Asmundsson, R., Pezard, P., Sanjuan, B., Henninges, J., Deltombe, JL., Halladay, N., Lebert, F., Gadalia, A., Millot, R., Gibert, B., Violay, M., Reinsch, T., Naisse, JM., Massiot, C., Azais, P., Mainprice, D., Karytsas, C., and Johnston, C. "High Temperature Instruments and Methods Developed for Supercritical Geothermal Reservoir Characterization and Exploitation The HiTI Project." *Geothermics*, 49, (2014), 90-98.
- Benoit, D., and Thompson, S. "Development and Testing of a Single-Ended Distributed Temperature Sensing System at the Beowawe, Nevada Geothermal Reservoir." *Geothermal Resources Council Transactions*, 22, (1998), 575-581.
- Bogatyrev, V.A., and Semjonov, S. "Metal-Coated Fibers." In Mendez, A., and Morse, T.F. editors, Specialty Optical Fibers Handbook, Academic Press, (2007), 491-512.
- Bolognini, G., and Hartog, A.H. "Raman-based Fibre Sensors: Trends and Applications." *Optical Fiber Technology* 19.6 (2013), 678-688.
- Dobson, P., Asanuma, H., Huenges, E., Poletto, F., Reinsch, T., and Sanjuan, B. "Supercritical Geothermal Systems A Review of Past Studies and Ongoing Research Activites." *Proceedings, 41st Workshop and Geothermal Reservoir Engineering*, Stanford University, Stanford, CA (2017).
- Duncan, W. J., France, P.W., and Beales, K.J. "Effect of service environment on proof testing of optical fibers." 7th ECOC, Copenhagen, Paper 4.5-1 (1981).
- Elders, W.A., Fridleifsson, G.O., and Saito, S. "The Iceland Deep Drilling Project: Its global Significace." *International Geothermal Conference*, Session 6, Reykjavik, Iceland (2003).
- Fernandez, A.F., Rodeghiero, P., Brichard, B., Berghmans, F., Hartog, A.H., Hughes, P., Williams, K., and Leach, A.P. "Radiation-tolerant Raman Distributed Temperature Monitoring System for Large Nuclear Infrastructures." *IEEE Transactions on Nuclear Science* 52.6 (2005), 2689-2694.
- Forster, A., and Schrotter, J. "Distributed Optic-Fibre Temperature Sensing (DTS): A New Tool for Determining Subsurface Temperature Changes and Reservoir Characteristics." *Proceedings, Twenty-First Workshop and Geothermal Reservoir Engineering*, Stanford University, Stanford, CA (1997).
- Kimura, A., Takada, E., Fujita, K., Takahashi, M., and Ichige, S. "Application of a Raman Distributed Temperature Sensor to the Experimental Fast Reactor JOYO with Correction Techniques." *Measurement Science and Technology* 12 (2001), 966-973.
- Lemaire, Paul J. "Reliability of optical fibers exposed to hydrogen: prediction of long-term loss increases." *Optical Engineering* Vol. 30 No. 6, 780-789 (1991).
- Massiot, C., Asmundsson, R., and Pezard, P.A. "Achievements and Ongoing Progress of the European HiTI Project: High Temperature Instruments for Supercritical Geothermal Reservoir Characterization and Exploitation." *Proceedings World Geothermal Congress*, Bali, Indonesia (2010).

- Noguchi, K., Shibata, N., Uesugi, N., and Negishi, Y. "Loss Increase for Optical Fibers Exposed to Hydrogen Atmosphere." Journal of Lightwave Technology Vol. LT-3 No. 2, (1985), 236-243.
- Normann, R.A., and Glowka, D.A. "Designing Logging Tools for Future High Entropy Geothermal Power." GRC Transactions, 38, (2014), 559-562.
- Palit, S., Challener, W., Lopez, J., Mandal, S., Xia, H., Jones, R., Craddock, R., Zao, L., Irshad, M., MacDougall, T.W., Sanders, P., Herbst, B., Villiger, B., Vo, S., Henfling, J., Lindblom, S., and Maldonado, F. "A Multi-Modality Fiber Optic Sensing Cable For Monitoring Enhanced Geothermal Systems." *Proceedings, Thirty-Seventh Workshop and Geothermal Reservoir Engineering*, Stanford University, Stanford, CA (2012).
- Palsson, B., Frioleifsson, G.O., and Elders, W.A. "Iceland Deep Drilling Project How to Handle the Worlds Hottest Goethermal Well?" *New Zealand Geothermal Workshop 2011 Proceedings*, Auckland, New Zealand (2011).
- Reinsch, T., and Henninges, J. "Temperature Dependent Characterization of Optical Fibres for Distributed Temperature Sensing in Hot Geothermal Wells." *Measurement Science and Technology*, 21, (2010).
- Reinsch, T., Henninges, J., and Asmundssson, R. "Thermal, Mechanical and Chemical Influences on the Performance of Optical Fibres for Distributed Temperature Sensing in a Hot Geothermal Well." *Environmental Earth Sciences*, 70, 8, (2013), 3465-3480.
- Sanders, P.E., and MacDougall, T.W. "Recent Developments in Fiber Optic Sensor Technology for High Temperature Well Monitoring." *GRC Transactions*, 33, (2009), 859-863.
- SEAFOM, "Measurement Specification for Distributed Temperature Sensing (SEAFOM-MSP-01)." http://www.seafom.com/index.php/documents/published-documents, (2016).
- Soto, M.A., Nannipieri, T., Signorini, A., Lazzeri, A., Baronti, F., Roncella, R., Bolognini, G., and Di Pasquale, F. "Raman-based Distributed Temperature Sensor with 1 m Spatial Resolution over 26 km SMF Using Low-repetition-rate Cyclic Pulse Coding." *Optics Letters* 36.13 (2011), 2557.
- Stoddart, P. R., Cadusch, P. J., Pearce, J. B., Vukovic, D., Nagarajah, C. R., and Booth, D. J. "Fibre Optic Distributed Temperature Sensor with an Integrated Background Correction Function." *Measurement Science and Technology* 16.6 (2005), 1299-1304.
- Stone, J., Chraplyvy, A.R., and Burrus, C.A. "Gas-in-glass—a new Raman-gain medium: molecular hydrogen in solid-silica optical fibres." *Opt. Lett.*, 7, (1982), 297-299.
- Wang, C., Drenzek, G., Majid, I., Wei, K., Bolte, D., Soufiane, A. "High-Performance Hermetic Optical Fiber for Downhole Applications." SPE 91042, (2004).
- Weiss, J. "Downhole geothermal well sensors comprising a hydrogen-resistant optical fiber." *U.S. Patent No.* 6,853,798 *B1*, (2005).